International Journal of Thermofluids 22 (2024) 100660

Contents lists available at ScienceDirect

International Journal of Thermofluids

journal homepage: www.sciencedirect.com/journal/international-journal-of-thermofluids

An investigation of thermal decomposition behavior and combustion parameter of pellets from wheat straw and additive blends by thermogravimetric analysis

Bidhan Nath [a,*], Guangnan Chen [a], Les Bowtell [b], Elizabeth Graham [c]

[a] School of Agriculture and Environmental Science, University of Southern Queensland, Toowoomba, QLD 4350, Australia
[b] School of Engineering, University of Southern Queensland, Toowoomba, QLD 4350, Australia
[c] Physical and Mechanical properties laboratory, Central Analytical Research Facility, Queensland University of Technology, Brisbane, QLD 4000, Australia

ARTICLE INFO

Keywords:
Combustion parameters
Wheat straw pellet
Thermogravimetric analysis
Derivative thermogravimetric analysis
Thermal behavior

ABSTRACT

This study investigates the intricate thermal decomposition behavior and combustion characteristics of two distinct types of wheat straw pellets (WSP) represented as T_1 (100 % wheat straw) and T_5 (70 % wheat straw; 10 % sawdust, 10 % biochar; 10 % bentonite clay). Through a thermogravimetric analyzer (TGA) the pellets undergo combustion under varying heating rates (5, 10, and 20 °C/min) in an air atmosphere, ranging from 25 to 1200 °C. Differential thermogravimetric and thermogravimetric analyses reveal four distinct stages of decomposition in the biomass components. The results indicate that the optimal combustion heating rate is 20 °C/min, resulting in the highest reaction rate (~50 %/min) and most substantial mass loss (~55 %) for both T_1 and T_5 pellets. Notably, the T_5 pellet demonstrates a lower ignition temperature (207 °C, at 20 °C/min) and higher burnout (457 °C at 10 °C/min) compared to the T_1 pellet, indicating its superior suitability for combustion. The combustion efficiency ranges from 61.0 to 99 % within the temperature range of 300 to 700 °C, similar to coal combustion. Additionally, thermodynamic properties (D_i, D_b, C, and S) suggest the promising potential of WSP as a bioenergy feedstock. Furthermore, T_1 pellets demonstrate higher ignition temperatures (T_i) than T_5, indicative of rapid combustion and lower energy potential. burnout temperatures (T_b) revealed intricate results in both scenarios. These findings hold significance for the design of gasification or combustion reactors and the industrial utilization of WSP biomass. The insights gathered from this study offer valuable guidance for designing and enhancing bioenergy systems and fostering sustainable practices in utilizing agricultural residues for energy production.

1. Introduction

Global warming and anthropogenetic CO_2 emissions have drawn great attention due to their substantial effects on the ecosystem and human civilization [1]. Therefore, global research and development efforts have been made to create alternative fuels to decrease fossil fuel use and reduce carbon dioxide pollution [2]. Biomass, as it grows, can fix atmospheric carbon dioxide [3]. In addition, biomass can be regarded as a carbon-neutral fuel and successfully minimizes carbon dioxide emissions when burned. Thus, worldwide attention is increasing to biomass-based fuel utilization [4]. When biomass is transformed as a source of bioenergy, it produces solid, liquid, and gaseous substrates. The biomass-to-bioenergy conversion types and products are varied due to inherent physiochemical properties.

In this study, we focused on investigating the thermal decomposition characteristics of wheat straw pellets. Wheat straw (WS) is a highly promising bioenergy waste due to its global ubiquity, wide availability, and lower cost, primarily from field crop cultivation [5]. Notably, wheat is the predominant grain industry crop in Australia. As of 2021/22, the average wheat yield in the country reached 36.3 million tonnes [6], which is estimated at 45.0 million tonnes of wheat residue as crop waste (with a grain and straw ratio= 1:1.3). Based on current assessments, WS residue holds an annual average energy potential of 146.52 TJ. Moreover, Australia has transitioned away from wood pellet manufacturing, using it as a renewable energy source [7]. Therefore, producing wheat straw pellets and characterizing their combustion properties are important for their industrial use as renewable energy sources.

The properties of biomass fuel are pivotal in determining its practical application. A systematic investigation of its properties is imperative to

* Corresponding author at: School of Agriculture and Environmental Science, University of Southern Queensland, Toowoomba, QLD 4350, Australia.
E-mail address: u1090250@umail.usq.edu.au (B. Nath).

https://doi.org/10.1016/j.ijft.2024.100660

Available online 16 April 2024

Nomenclature

BC	Bentonite Clay
BD	Bulk Density
BioC	Biochar
C	Flammability index
DTG	Derivative Thermogravimetric
D_i	Ignition index
D_b	Burnout index
FC	Fixed Carbon
HHV	Higher Heating Value
m	Mass
MC	Moisture content
n	Combustion efficiency
R_p	Maximum weight loss rate
R_v	Average weight loss rate
S	Combustibility index
SD	Sawdust
TG	Thermogravimetric
TGA	Thermogravimetric Analyser
T_b	Burnout temperature
T_i	Ignition temperature
T_p	Peak temperature
t_b	Burnout time
t_i	Ignition time
t_p	Peak reaction time
WS	Wheat Straw
WSP	Wheat Straw Pellet
VM	Volatile Matters
β	Heating rate

utilize biomass in bioenergy effectively. Fuel selection, consumption rates, and reactor design are all contingent on the biomass's thermal behavior and combustion characteristics [8]. In this context, key characteristics associated with the thermal decomposition of the fuels, including ignition temperatures (T_i), burnout temperatures (T_b), flammability index (C), and combustibility index (S), hold significant importance. Ignition is the lowest temperature at which a fuel can spontaneously ignite in an environment devoid of an external heat source [9]. Understanding this parameter is important for ensuring safety during storage and transportation, especially when used as an industrial fuel. Conversely, the burnout temperatures indicate when the fuel is almost entirely depleted, serving as a measure of its burn response. Higher burnout temperatures indicate fewer combustible components within the fuel [10]. Additionally, the flammability and combustibility indices offer valuable insights into combustion performance. As suggested by Chen, Liu [11], a higher S value signifies a swifter and more intense combustion process, while a higher C value suggests greater combustion stability [12]. Overall, assessing combustion behavior and properties is essential for industrial applications.

The operational conditions under which fuel is utilized notably impact its thermal characteristics. Studies by, Kok and Özgür [13] and [14] demonstrate that heating rates significantly influence ignition temperatures of biomass fuels like miscanthus and rice husk. Additionally, Pan, Jia [15] highlight how identification methods, like the intersection method, can significantly impact combustion yield. while Ma, Li [16] explored the influence of catalysts on ignition and burnout temperatures in rice and wheat straw, they did not delve into combustion indices or thermal breakdown. Di, Wang [17] observed similar effects of catalysts on coal combustion. Researchers like Petrovič, Stergar [18] and Kardaś, Kluska [19] have successfully employed thermogravimetric analyzers (TGA) to assess the thermal performance and co-combustion behavior of blends like wheat straw and sewage sludge, revealing positive interactions at high temperatures [20]. Furthermore, Raza, Mustafa [21] used a waste-to-waste approach using TGA alongside FTIR, XRD, and DSC to isolate cellulose from date palm waste, highlighting the versatility of TGA in biomass research.

While some research has studied wheat straw pellets as a fuel, a comprehensive understanding of their behavior with different additives is lacking. In particular, detailed thermogravimetric analysis (TGA) of these pellets is scarce. Previous studies might not have investigated the full spectrum of additives and their impact on how wheat straw pellets decompose and combust, including efficiency and thermal stability. To address this gap, this research will employ TGA to meticulously examine wheat straw pellets' thermal decomposition and combustion characteristics containing various additives. By systematically analyzing these factors, this study aims to bridge the current knowledge gap and provide valuable insights. This, in turn, could help industries select the most appropriate heating methods and rates, ultimately leading to more accurate combustion parameters for biomass applications.

A large amount of scientific literature is available on wheat straw co-combustion, with most studies focusing on combining coal and wheat straw [5,22–25]. While this co-combustion presents a promising approach that offers a clean and efficient way to utilize coal, it raises concerns about nitrogen oxide (NOx) and sulfur dioxide (SO2) emissions [26,27]. Some research has explored co-combustion with alternative biomass sources like torrefied reeds and poplar wood, but these studies have not addressed key factors like combustion efficiency and indicators [28] and [29]. Other investigations have focused on specific aspects like decomposition behavior during burning or pellet characteristics, without examining overall combustion parameters [30] and El-Sayed and Khairy [31]. Recent work by Kumar and Nandi [5] delves into the combustion characteristics of various blends, including wheat straw, highlighting the ongoing exploration in this area [32]. Gageanu, Cujbescu [33] they have manufactured various pellets using individual additives (wheat straw and rapeseed stalk) and combinations of additives. They observed that pellets made with individual additives had lower bulk density and higher ash content than those with multiple additives. Similarly, Emami, Tabil [34] they obtained comparable results with pellets made from individual additives, noting that combining multiple additives could enhance bulk density, relaxed density, durability, and specific energy content compared to pellets blended with a single additive. While research has explored individual additives for wheat straw pellets (WSP), a fundamental gap exists in understanding how these additives interact with each other and the WSP itself. This combined influence on thermal properties remains largely unknown. Investigating these interactions is essential, as additives might exhibit synergistic or antagonistic effects that significantly impact combustion behavior. Understanding WSP decomposition and combustion is paramount for designing efficient biomass energy systems. This research addresses this challenge by examining how different additive combinations (Bentonite clay, Sawdust, and Biochar) influence thermal behavior. By scrutinizing these interactions and their impact on decomposition and combustion, the study offers valuable insights for optimizing pellet composition. This focus on additive interaction is the key innovation of this research, with the potential to dramatically improve biomass-to-energy conversion efficiency.

Biomass thermal conversion to energy [35] via combustion involves intricate physiochemical mechanisms. TGA is a powerful and widely used tool for measuring the thermogravimetric (TG) profile, indicating mass changes over time or in response to temperature variations [36]. In addition, TGA provides valuable insights into various combustion characteristics due to its versatile application [37]. The thermogravimetric (TG) and derivative thermogravimetry (DTG) curves, derived from TGA, serve as valuable tools for observing the temperature-time

relationship in reaction rates. Furthermore, the TG/DTG profile aids in determining the thermokinetic properties of WSP. These properties are vital in understanding solid fuel combustion and are integral to large-scale industrial reactors' design, development, and operation [38]. Therefore, the primary objectives of this present study are twofold: (a) to ascertain the thermal decomposition behavior and (b) to determine burning factors (ignition temperature, burnout temperature, flammability indices, and comprehensive combustion index). These parameters could use as input data in Computational Fluid Dynamics (CFD) modeling for designing a reactor and analyzing the pellets' energy conversion [39].

2. Materials and methods

2.1. Test sample and sample preparation

Two wheat straw pellets (T_1 and T_5) were made and used in this study with different material combinations (Table 1). In this work, two types (treatments) of pellets were used for qualitative analyses. This research followed the published article regarding the proportion of blenders used and their material characteristics (moisture content and particle size). According to Pradhan, Mahajani [40], the moisture range is 15 to 23 %, and a particle size of less than 6.5 mm is required for pellet processing. In addition, Nazemi, Safavi [41] suggested that 20 % of sawdust with wheat straw can enhance pellet strength. Also, additives proportion of 0.5 to 5 % (total mass fraction) can improve pellet quality [42]. Therefore, the present research considered the raw material moisture content to be around 20 %, with particle size not bigger than 2 mm. Moreover, the bentonite clay, sawdust, starch, glycerol, and biochar ratio were all set at a 10 % (weight basis) level. Furthermore, in pellet production, used biochar enhances the higher heating value, bentonite functions as a binding agent, while sawdust contributes to the uniform compaction of the structure.

This investigation focused on wheat straw pellets (T_1), identified from a previous study as having the lowest quality rating [43]. Seven pellet types were created, with only T_5 meeting the established suitability criteria outlined by ISO standards [44]. Hence, for a comprehensive analysis, these specific pellets were chosen for examination. These cylindrical solid fuels, comprised of wheat straw with and without additives, required grinding prior to TGA analysis. However, it was needed to grind the samples in preparation for the Thermogravimetric analyzer (TGA). The process increased their surface area [43] and enhanced the conversion efficiency [45].

Subsequently, the samples underwent a 24 h drying period in an oven set at 105 °C, followed by grinding to achieve an average particle size of 1 mm (Fig. 1). The resulting crushed sample was then sieved to maintain uniform particle sizes. A dummy test was also conducted at each heating rate to mitigate potential systematic errors and establish baseline information. To ensure precision in the experiment results, an equal sample size (weight) was utilized for each treatment [32], with an initial weight of 50 mg for each run. However, it is essential to note that the TGA pan had a sample holding capacity of only 8.75~9.75 mg. To uphold accuracy, the experiment was replicated thrice, ensuring precision and reproducibility in the analysis. The mean value of the collected data was utilized for the current study.

Table 1
Experimental sample types and their physical characteristics.

Pellets	Combinations (Weight proportion)	Average length, mm	Mean diameter, mm	Bulk density, Kg/m
T_1	WS (100 %)	22.0 ± 2.32	8.21 ± 0.53	244.79 ± 15.45
T_5	WS (70 %) + SD (10 %) + BC (10 %) + BioC (10 %)	37.0 ± 1.32	8.13 ± 0.12	607.40 ± 8.11

Note: WS= Wheat straw, BC= Bentonite clay, SD= Sawdust and BioC= Biochar.

2.2. Experimental protocol

Accurately determining wheat straw and additive pellets' thermal decomposition behavior and combustion parameters through thermogravimetric analysis (TGA) hinges on adhering to established industry standards and protocols [46]. This meticulous process involves several well-defined steps: sample preparation, TGA analysis, data collection, and in-depth analysis of the results (Fig. 2). First, researchers meticulously prepare the wheat straw and additive blends for TGA compatibility. The experiment then proceeds within the TGA instrument under precisely controlled conditions. A standardized procedure guarantees consistent data collection, meticulously recording the sample's mass change as the temperature rises. Finally, this data undergoes rigorous analysis to extract crucial parameters like activation energy and reaction kinetics. Furthermore, strict adherence to safety protocols during experimentation is paramount to ensure the researcher's well-being.

2.3. TGA experiments

TGA is the foremost technique for probing into the decomposition behavior [21] and kinetics of carbonaceous materials with both temperature (non-isothermal) and time (isothermal) [47–49]. In this study, the STA 449F3 Jupiter TGA (Erich NETZSCH GmbH & Co. Holding KG, Germany) was used to measure and record the dynamics of the constant mass loss of the samples with as temperature and time increased [50]. The feedstock underwent combustion in the control zone under a pressure of 0.1 MP, with air serving as the carrier gas maintained at a steady 50 ml/min flow rate [51]. The TG and DTG data for the current investigation were obtained using cutting-edge kinetic software NETZSCH Proteus 8.0 (NETZSCH-Gerätebau GmbH) for WSP combustion under dynamic conditions. This NETZSCH software enables the analysis of temperature-dependent chemical processes [52].

2.4. Thermogravimetric analysis

The samples' combustion reaction rate was determined by analyzing the remaining mass distribution and the derivative of mass loss data. Moreover, the mass loss data, depicted in TG curves, were utilized to determine pseudo-component degradation (lignin, hemicellulose, and lignin) [53]. In contrast, the DTG profiles are assessed by DTG profiles [54]. To refine the TGA data, a moving average trend line was applied to mitigate any noise interference, a common strategy in TG data examination [55,56].

The TG/DTG data were collected using the integrated computer at linear heating rates of 5, 10, and 20 °C/min, covering a temperature range from 25 to 800 °C. These specific heating rates and temperature ranges have been widely adopted in numerous experiments to assess the kinetic properties of various biomass samples [57,58].

2.5. Combustion characteristic parameters

The combustion efficiency was assessed using the following eight parameters and indices [12,59].

(i) ignition temperature (T_i), (ii) burning temperature (T_b),

(iii) maximum weight loss rate ($-R_p$), (iv) average weight loss rate ($-R_v$),

(v) combustibility index (S), (vi) ignition index (D_i),

(vii) flammability index (C). (viii) burnout index (D_b)

2.5.1. Ignition and burnout temperatures

Examining fuel qualities is important in assessing fuel selection, consumption rates, reactor design, and successful application [60]. Within this context, ignition and burnout temperatures are pivotal properties in bioenergy production.

Various methods, including intersection, conversion, and deviation, can determine a fuel's ignition and burnout temperatures [61]. Under a

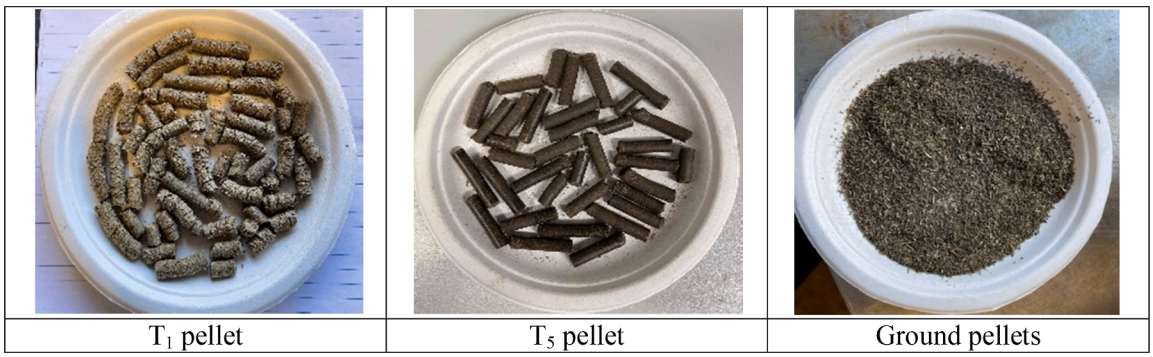

Fig. 1. Photographic illustration of experimental material: wheat straw pellet.

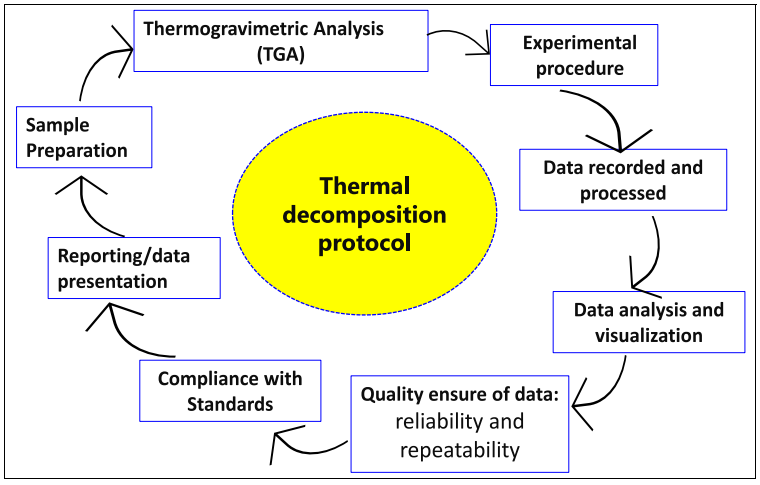

Fig. 2. Standard thermogravimetric analysis protocol for wheat straw pellets.

consistent heating rate, the intersection technique determines the ignition and burnout temperatures by analyzing TGA and DTG combustion profiles [62]. One of the key advantages of this method lies in its straightforwardness [63]. Fig. 2 visually represents the intersection method for both ignition and burnout temperatures.

Lu [55] has conducted a comprehensive review of several methods (Fig. 2). For the ignition temperature, determined through the intersection method, the following steps are followed:

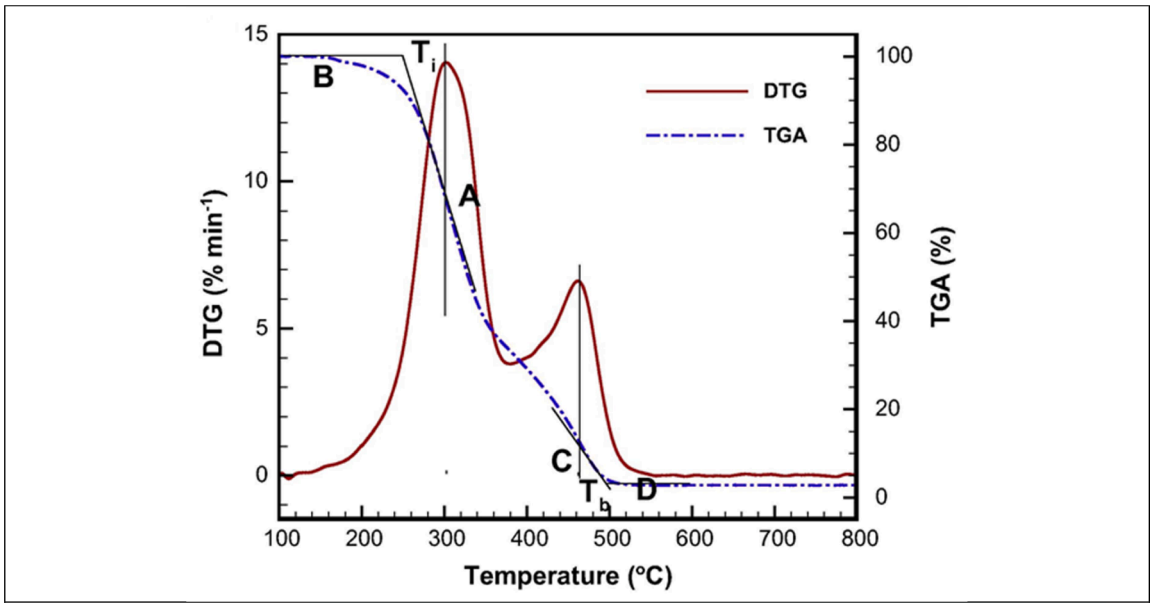

Fig. 3. Intersection method for determining ignition (T_i) and burnout (T_b) temperatures [55].

- At Point A, a vertical line is drawn from the first peak of the DTG curve, representing the peak value in the DTG curve (Fig. 3). This marks the beginning of devolatilization point B.
- On the TGA curve, a tangent is drawn from A, and a horizontal line is extended from B.
- The ignition temperature (Ti) is established at the intersection of these two lines.

When calculating the burnout temperature of biomass, the single peak of a DTG curve was used [64]. It is worth noting that when air is the carrier gas, certain biomass species show two distinct peaks in their DTG plots [65]. In such cases, the second peak is used to determine the burnout temperature rather than the first. Point C on a TG curve, where a vertical line from the second peak of the DTG curve intersects the TGA curve, is shown in Fig. 3. As the TGA curve progresses to point D, it stabilizes. The burnout temperature (T_b) is established at the intersection of a tangent drawn from the TGA curve at C and the horizontal line extending from D.

2.5.2. Combustion efficiency indices

The T_i, T_b, R_p, and R_v parameters were derived from the TG/DTG profile, whereas S, D_i, D_b, and C were calculated using the equations provided in references [50] and [51,66,67]. Higher flammability and combustibility indices indicate enhanced combustion and ignition performances, respectively—the flammability index, as outlined in the reference [68].

$$S = \frac{-R_p \times -R_v}{T_i^2 \times T_b} \quad (1)$$

$$D_i = \frac{-R_p}{t_i \times t_p} \quad (2)$$

$$D_b = \frac{-R_p}{\Delta t_{1/2} \times t_p \times t_b} \quad (3)$$

$$C = \frac{-R_p}{T_i^2} \quad (4)$$

$$n = \frac{m_{110} - m_e}{m_{100} - m_t} \times 100\% \quad (5)$$

Whereas:

R_p= maximum mass loss rate,%/min
R_v= average mass loss rate,%/min
C= flammability index, 10^{-4}%/(min.°C^2)
$\Delta t_{1/2}$= the time interval of DTG/DTG_{peak}= 0.5
n= combustion efficiency,%
m_{110}= mass loss at 110 °C,%
m_e=mass loss at any temperature,%
m_t= mass loss end temperature,%
S= comprehensive combustion index, 10^{-7} %^{2}/(min^2.°C^3)
T_i= ignition temperature, **°C**
T_p= peak temperature, **°C**
T_b= burnout temperature, **°C**
t_i = ignition time, min
t_p = peak reaction time, min
t_b = burnout time, min
D_i= ignition index, 10^{-2} %/min^3
D_b = burned-out index, 10^{-2} %/min^4

3. Results and discussion

3.1. Physicochemical analysis

The chemical analysis of materials is detailed in Table 2 and was conducted by established standard techniques, as outlined in the previous study [69]. Typically, materials with higher volatile content are more readily ignitable. However, a higher ash content may adversely affect thermal degradation stability and slow the burning rate [70]. Notably, the volatile content of T_1 (75.61 %) was higher than that of T_5 (53.03 %). This discrepancy in volatile content and the combustible fuel ratio indicated that T_1 pellets were poised to burn and ignite more efficiently than T_5 [71]. However, the fixed carbon (FC) contents stood at 11.10 % for T_1 and 31.60 % for T_5 (as shown in Table 2), with T_5 having a significantly higher ash content of 11.87 % in contrast to T_1 at 7.09 %. Furthermore, the higher heating value (HHV) of T_5, measured at 19.06 MJ/kg, surpassed that of T_1, recorded at 17.024 MJ/kg. Notable, the HHVs of the pellet were higher than those of corn cob (16.90 MJ/kg), rice straw (16.78 MJ/kg), barley straw (15.70 MJ/kg) [72], and pine sawdust (16.81 MJ/kg) [73]. However, they were lower than those of liquor-industry wastes (19.53 MJ/kg) [74] and sub-bituminous coal (25.31 MJ/kg) [75]. These findings underscore the significant potential of wheat straw residues as an available biofuel source for combustion and emphasize the important considerations required for practically utilizing this residue for combustion.

The nitrogen (N) contents of T_1 (0.56 %) and T_5 (0.72 %) closely resembled those of corn cob (0.70 %) and rice straw (0.63 %) [72], but were lower than those found in lignite (1.55 %) [76], sub-bituminous coal (1.59 %), and bituminous coal (1.50 %) [75]. At the same time, T_1 (0.11 %) and T_5 (0.21 %) had low sulphur (S) contents compared to maize cob (1.30 %), beech wood (0.70 %) [72], lignite (0.89 %) [76], sub-bituminous coal (7.14 %), and bituminous coal (0.56 %) [75]. So, it is worth noting that the nitrogen and sulphur contents of the WSP were notably lower than those of coal, sludge, and specific biomass. This indicates the potential for reduced emissions of nitrogen oxides (NO_x) and sulphur oxides (SO_x) during the combustion of WSP. Overall, the comprehensive analysis of the physicochemical properties of wheat straw pellets, particularly in comparison to coal and other biomass varieties, reveals promising combustion, kinetic, and thermodynamic characteristics. This suggests a strong potential for further research and development of WSP as biofuel.

As a general observation, wheat straw biomass typically exhibits higher ash content than other forms of biomass such as woody, solid (pellet, briquette), etc. [69]. However, the ash content of WSP was lower than coal's (22.24 %) [77]. These findings suggest the importance of post-combustion residue treatment in practical applications.

3.2. Decomposition characteristics of WSP

The thermal properties of wheat straw pellets (T_1 and T_5) were assessed through combustion processes conducted in a TGA under an air atmosphere. The TG/DTG profiles for both T_1 and T_5 pellets are shown in Figs. 3–10. Thermal degradation of each wheat straw pellet can be

Table 2
Proximate and ultimate analysis results of wheat straw pellets.

Sample/pellets	Proximate analysis,%, as received, dry basis				Ultimate analysis,%, dry basis					Calorific value (HHV), MJ/kg
	MC	VM	FC	Ash	C	H	N	S	O*	
T_1	6.20	75.61	11.10	7.09	44.32	4.90	0.56	0.11	50.11	17.02
T_5	3.50	53.03	31.60	11.87	45.87	6.30	0.72	0.21	46.90	19.06

Note: MC= Moisture content; VM= Volatile matters; FC= Fixed carbon; * by difference.

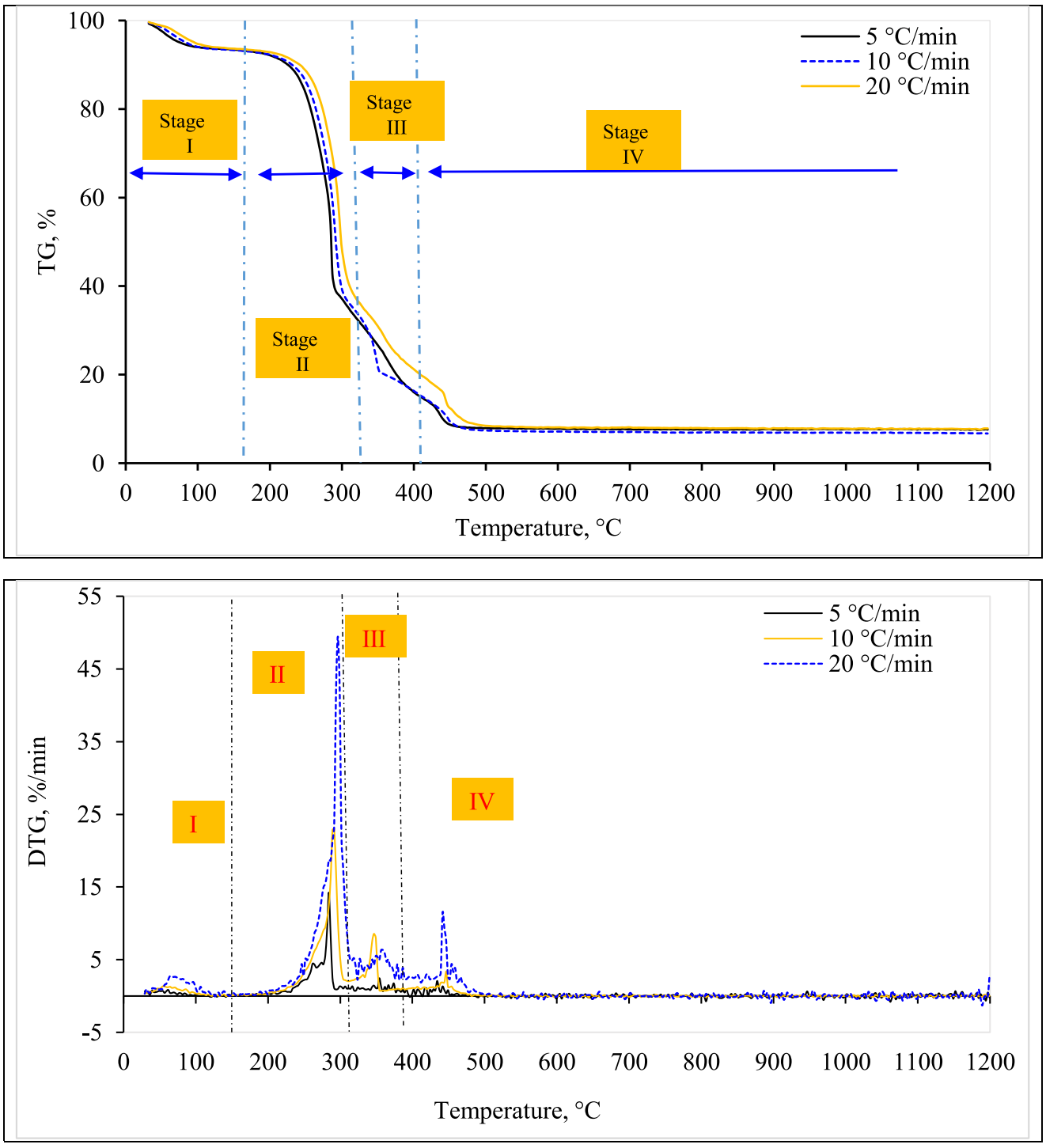

Fig. 4. Combustion profile of T_1 pellets at different heating rates: (a) TG curve and (b) DTG curves.

categorized into four distinct phases or regions, as indicated by the numbered sections in Figs. 3 and 4. The classification aligns with findings supported by previous research [54,66,78]. Given that the primary components of the samples encompass hemicellulose, cellulose, lignin, and extractives [79], these four stages correspond to their release and subsequent decomposition, as detailed in Table 3. Notably, the DTG profile exhibits a central peak accompanied by several side peaks. These side peaks originated from hemicellulose, lignin, and other substances, whereas the combustion of cellulose generates a distinct and pronounced peak [80].

3.2.1. Analysis of TG/DTG profiles for pellet T1

- ***At a heating rate of 20 °C/min***

The TG/DTG profile at a heating rate of 20 °C/min is presented in Fig. 3. In the initial Stage (I), the temperature ranges from 25 to 172 °C, with a peak DTG value of 2.66 %/min occurring at 72 °C. At this 20 °C/min heating rate, the highest recorded mass loss in this stage was 7 % (Table 4). This phase primarily involves the release of moisture from the biomass cellular structure and its surface, a phenomenon associated

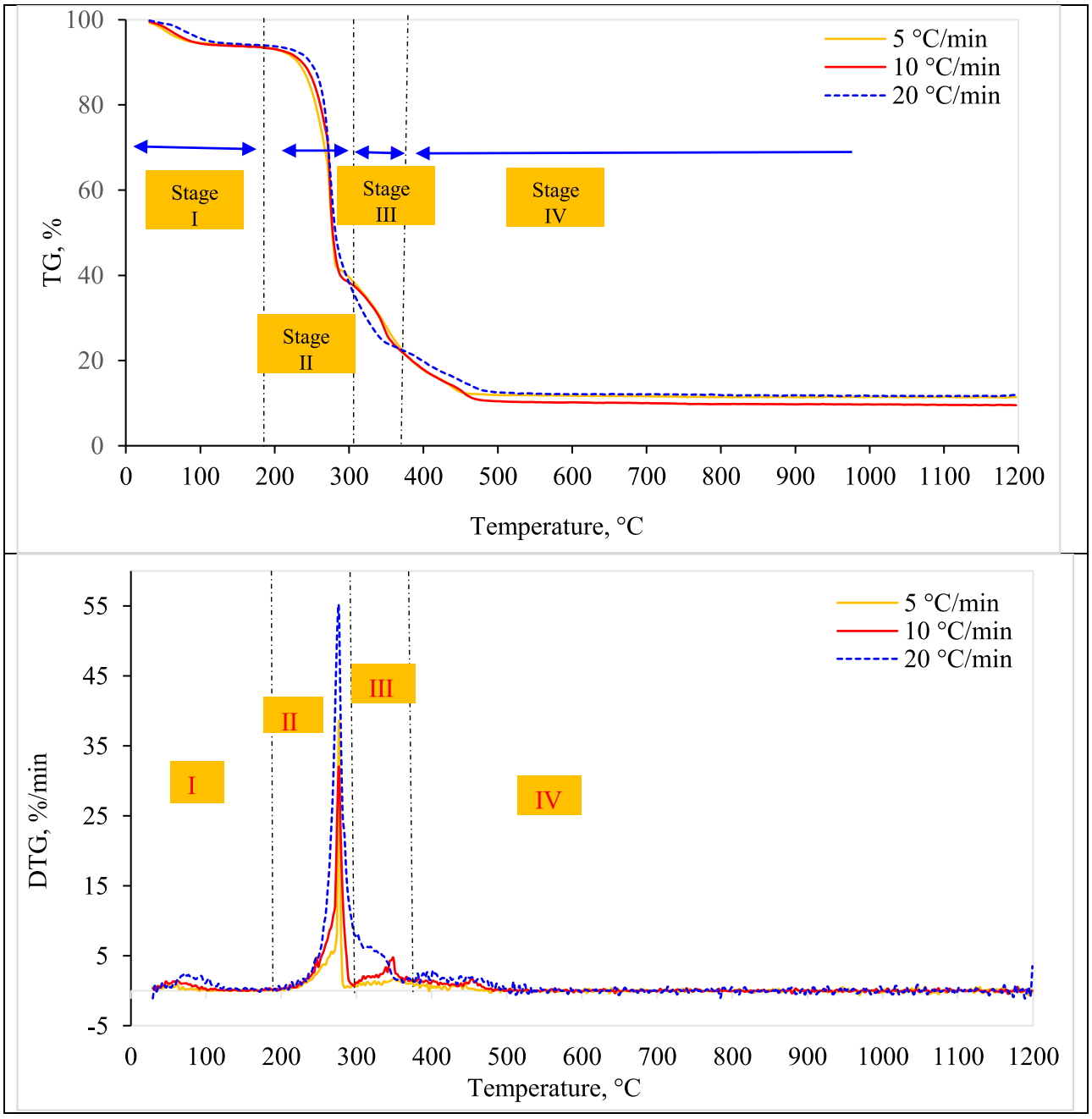

Fig. 5. Combustion profile of T_5 pellets at different heating rates: (a) TG curve and (b) DTG curves.

with the initial combustion stage [82]. As the sample is heated, moisture evaporates and escapes, resulting in a marginal reduction in mass.

The subsequent stage (II) covers a temperature range from 172 to 332 °C, exposing a substantial release of volatiles and a significant mass loss. This finding is supported by the work of Xu [83]. Notably, this second stage, termed oxidative degradation, is related to the decomposition of hemicellulose and cellulose. The peak DTG value for this stage was 49.45 %/min. The sample undergoes more rapid and thorough combustion in this phase, leading to the most significant weight loss of 54.15 % at a peak temperature of 297 °C (Table 4). This high mass loss is attributed to the highest volatile content at this stage [66].

In the third Stage, there was an overall weight loss of 22.72 %, with a peak temperature recorded at 357 °C (Fig. 4). This stage, also known as devolatilization, saw weight loss primarily attributed to the volatile matter and fixed carbon contents. Therefore, the third stage represents lignin and char's most substantial thermal degradation. The temperature variation for this stage was 332 to 409 °C, with the highest reaction rate reaching 6.33 %/min (Table 4). These findings align with other authors' reports, even when utilizing different biomass types [84]. In the final combustion phase (IV), inorganic materials, residual lignin, and char underwent combustion and stabilization [71]. This division also marked the formation of the final char, which eliminated secondary gases. The temperature at which the maximum weight loss (9.42 %) of lignin occurred was 442 °C, and the temperature range for this step was from 409 to 1200 °C.

- ***At a heating rate of 10 °C/min***

In Fig. 4, the TG/DTG curves are displayed. In this instance, four stages make up the thermal degradation combustion process. The initial Stage (I) observed the temperature ranging from 25 to 172 °C, resulting

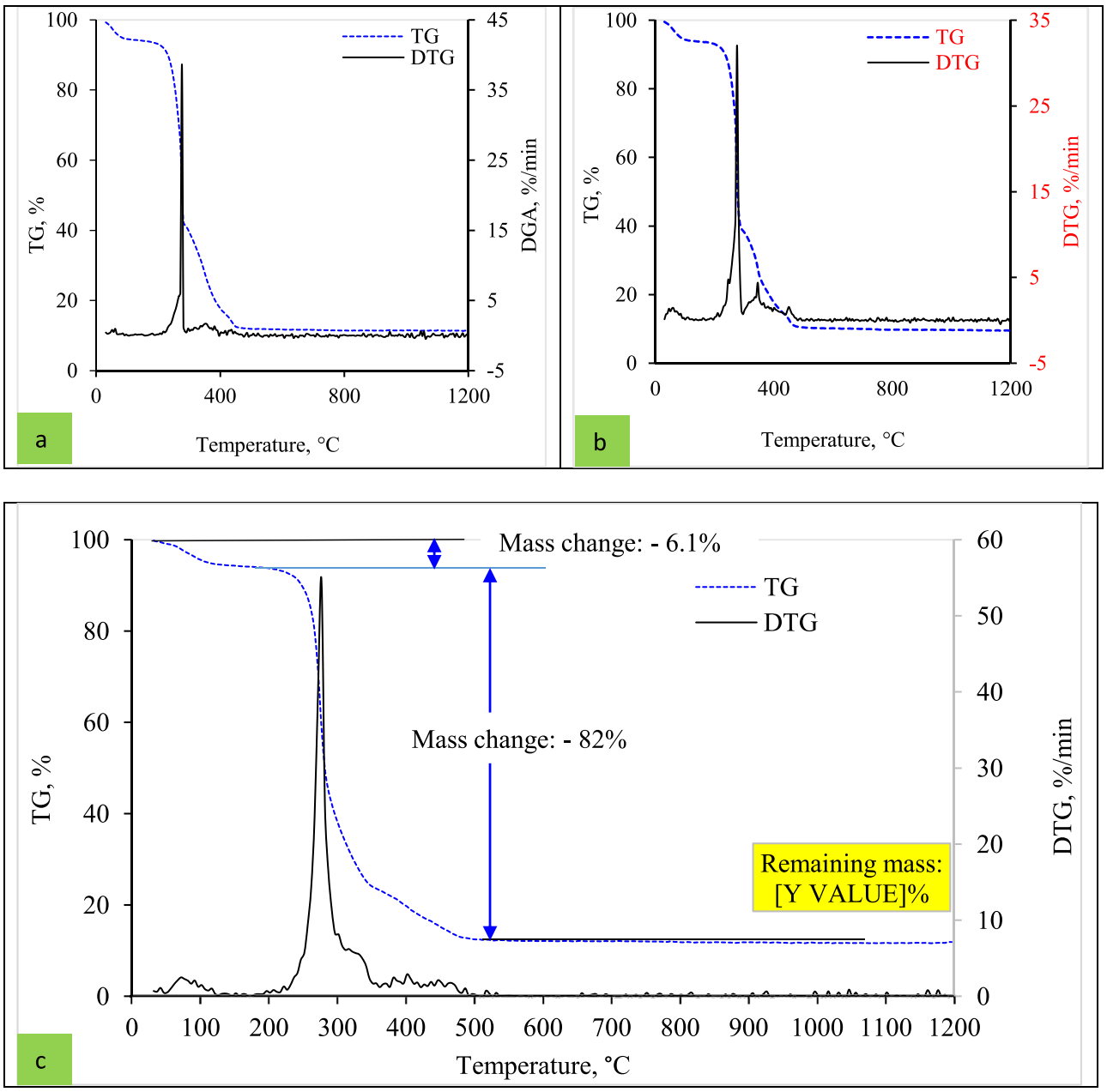

Fig. 6. TG and DTG curves for T_5 pellets combustion at a constant heating rate (a) 5 °C/min; (b) 10 °C/min and (c) 20 °C/min.

in a weight loss of 6.66 %. This can be attributed to the evaporation of moisture from the WSP. The second stage (II), characterized by the thermal degradation of hemicellulose, exhibits a substantial mass loss of 56.64 % and occurs within the temperature range of 172 and 332 °C. The third region (III), with a temperature variation of 332 to 409 °C, corresponds to the breakdown of cellulose, resulting in a weight loss of 15.74 % and the highest recorded reaction rate of 8.58%/min. This observation is supported by Rahib, Elorf [78], who obtained similar results using the Argan nutshell as biomass. The final stage (IV) involves a weight loss of 13.1 % and entails lignin degradation between 409 and 1200 °C. Lignin decomposes slowly within this temperature range due to its complex structure composition. At 1200 °C, the remaining sample accounted for 7.86 % (Table 4).

- ***At a heating rate of 5 °C/min***

The thermogravimetric profile (TG/DTG) is shown in Fig. 4. In this scenario, the combustion process of biomass thermal degradation consists of four zones. The mass loss at the first Stage (I) was 6.96 %, observed between 25 and 172 °C, which might be the evaporation of moisture from the wheat straw pellet. At temperatures between 172 and 332 °C, the second stage, which involves the heat breakdown of hemicellulose and has a mass loss of 60.13 % and a quick reaction rate (DTG_{max}) of 9.02 %/min, can be seen. The third stage, which corresponds to the breakdown of cellulose, causes a DTG_{max} of 1.51 %/min within the temperature range of 332 to 409 °C. In the final Stage (IV), there is an 8.23 % mass loss as lignin undergoes breakdown between 409 and 1200 °C. This observation is corroborated by Liu, Pang [85], who obtained similar results using different biomass (corn straw powder, poplar wood chip and rice husk). Post-combustion, the TG/DTG profiles tended to flatten, resulting in a remaining residue content of 7.6 % (Table 4).

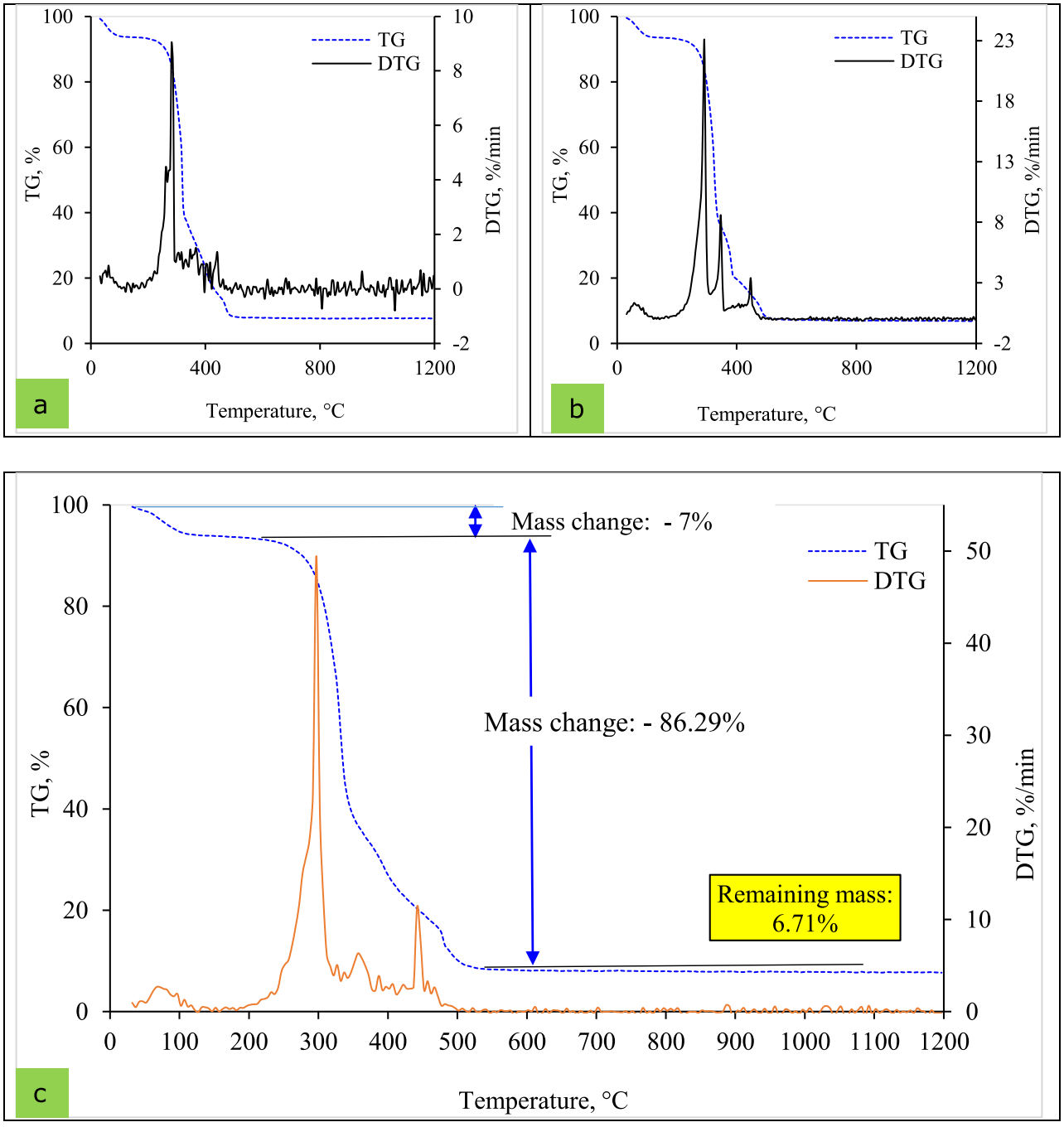

Fig. 7. TG and DTG curves for T_1 pellets combustion at a constant heating rate (a) 5 °C/min; (b) 10 °C/min and (c) 20 °C/min.

3.2.2. Analysis of TG/DTG profiles for pellet T5

- ***At a heating rate of 20 °C/min***

The DTG profile of the T_5 pellet was classified into four distinct stages (Fig. 5). The initial Stage (I), encompassed the range of 25 and 194 °C, where the initial combustion occurred. Within this zone of moisture loss, the highest DTG recorded was 2.49 %/min, occurring at a peak temperature of 72 °C, resulting in a mass loss of 6.1 %. The peak in the region signifies the degradation of hemicellulose (Table 5). The subsequent stage (II), across temperatures from 194 to 297 °C, saw the most significant decomposition, with an overall weight loss of 60.11 % and a peak temperature of roughly 277 °C. The maximum reaction rate in this region was 54.75 %/min, indicating the decomposition of primary cellulose and partial decomposition of hemicellulose and lignin at a heating rate of 20 °C/min. Therefore, the sample experienced rapid combustion within this oxidative region, a finding that aligns with the research of Xie, Wei [86].

On the other hand, stage III represents the devolatilization of a sample occurring within a temperature variation of 297 to 384 °C (Fig. 5). The maximum reaction rate, at 6.69 %/min, was reached at a peak temperature of 307 °C, resulting in a weight loss of 11.72 %. Gao, Yang [87] noted that primary combustion primarily occurs in stages II and III. Moving into phase (IV), the region signifies char combustion and the removal of secondary gases across temperatures from 384 to 1200 °C. Hameed, Naqvi [88] and Qureshi, Khushk [89] mentioned that lignin decomposes at maximum temperatures ranging from 500 to 900 °C. Within this stage IV, the highest reaction rate recorded was 2.9

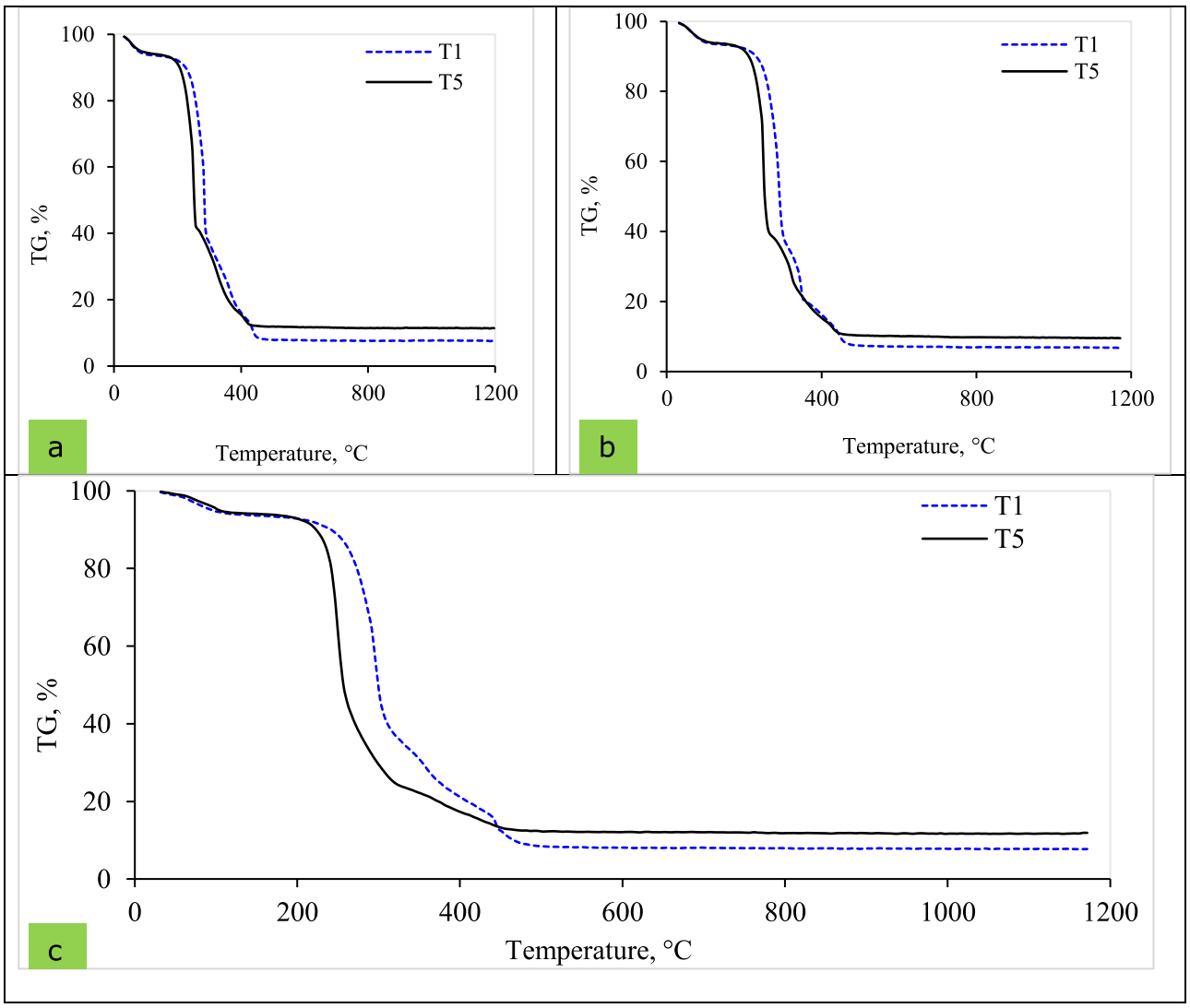

Fig. 8. Comparison of T_1 and T_5 pellets based on TG curves at a constant heating rate (a) 5 °C/min; (b) 10 °C/min and (c) 20 °C/min.

%/min, occurring at a peak temperature of 407 °C and resulting in a mass loss of 10.17 % (Table 5). Also, in this final stage, the combustion of hemicelluloses and cellulose was almost completely burned, while lignin was the predominant component. Therefore, the sample weight decreased, albeit with a smaller magnitude than the second and third phases. The DTG curves also tended to level off, a finding consistent with the research of Liu, Pang [85]. Consequently, after this process, the remaining portion of the sample accounted for approximately 11.9 % at a temperature of 1200 °C for a 20 °C/min heating rate.

- ***At heating rates of 10 °C/min***

The TG/DTG profile for the T_5 pellet at a heating rate of 10 °C/min is shown in Fig. 5. In the second stage (II), a notable peak reaction rate of 56.59 %/min was observed at a temperature of 347 °C. Following the combustion, the residual mass was 11.39 % (Table 5). Interestingly, in a study conducted by Sait, Hussain [90] investigating the pyrolysis and combustion kinetics of Date Palm biomass, a similar TG profile was observed, even though the biomass was different. This correlation highlights a consistent trend in thermal behaviour across distinct biomass sources.

- ***At heating rates of 5 °C/min***

Fig. 5 presents the thermogravimetric profile (TG/DTG) for T_5 pellets regardless of heating rates. It is evident from the figure that in region II, the highest mass loss was 55.08 % for the 5 °C/min heating rate, with peak temperatures reaching 277 °C. Post-combustion, the residual content stood at 11.39 % for 5 °C/min (Table 5). These findings closely align with other agricultural wastes such as wheat straw and groundnut stalk [91]. This similarity indicates a consistent pattern in the thermal behaviour of these biomass materials.

3.3. *Effect of heating rate on TG/DTG profile*

The influence of heating rate on the combustion behavior of WSP-both T_1 and T_5 at 5, 10, and 20 °C/min is detailed in Tables 4 and 5. The results indicate that varying the heating rate from 5 to 20 °C/min did not significantly alter the temperature ranges within the TG/DTG profiles. Nevertheless, an increase in heating rate did lead to shifts in peak temperature, resulting in changes in mass loss and maximum reaction rates across all treatments and heating rates. This observation aligns with the findings of Asadieraghi and Daud [92], who noted that higher heating speeds accelerated the decomposition rate, mirroring the outcomes of the current study.

For the T_1 pellet, in region III, peak temperatures were recorded at 357, 347, and 367 °C for heating rates of 20, 10, and 5 °C/min, respectively. Conversely, in region II, the DTG_{max} values were 9.02,

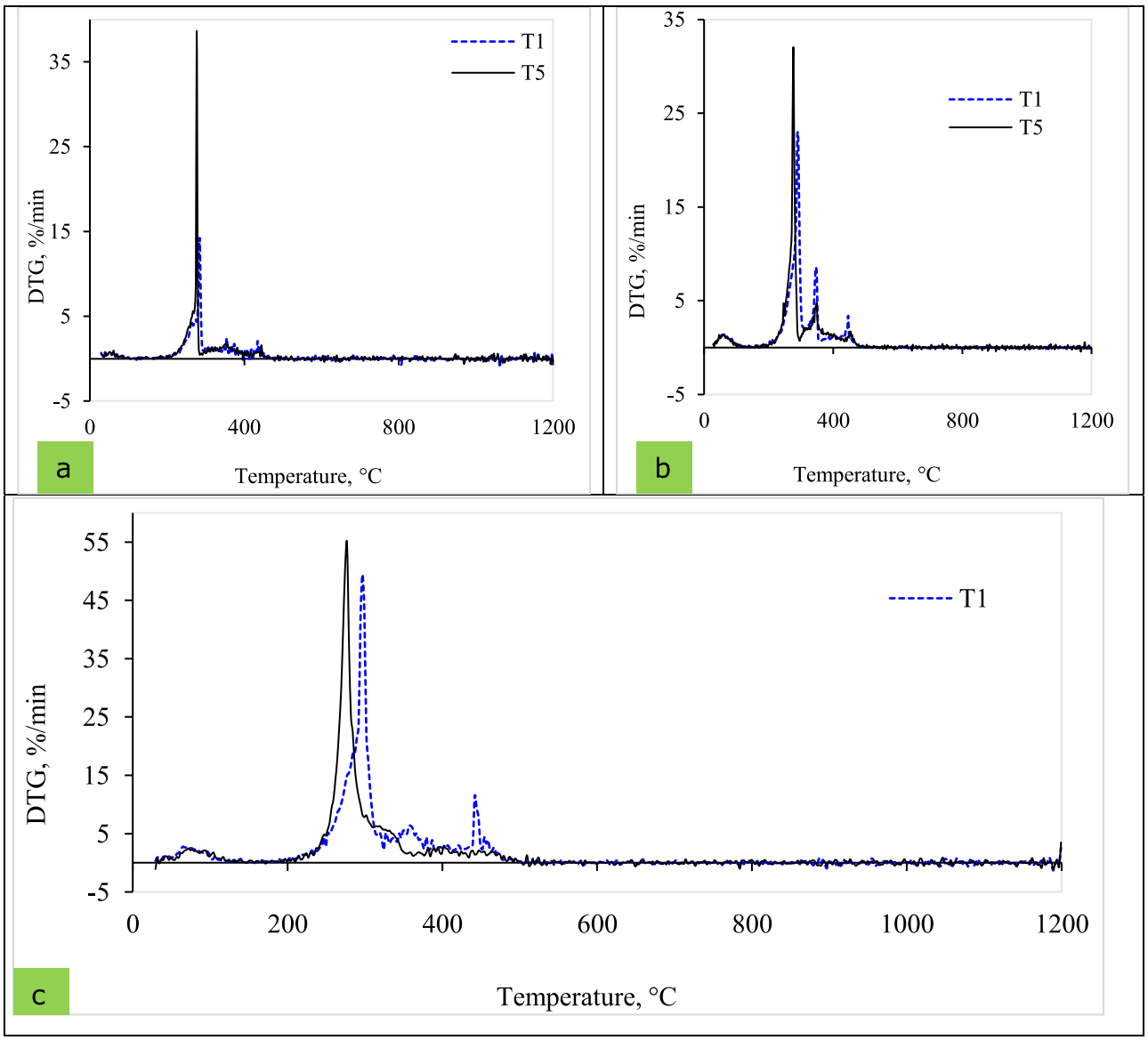

Fig. 9. Comparison of T_1 and T_5 pellets based on DTG curves during combustion at a constant heating rate (a) 5 °C/min; (b) 10 °C/min and (c) 20 °C/min.

22.99, and 49.45%/min for heating rates of 5, 10, and 20 °C/min, respectively (as outlined in Table 4). Regarding T_5 pellets, the average mass loss for the first Stage (I) was 6.1, 6.7, and 6.64 % at heating rates of 5, 10, and 20 °C/min, respectively. Following combustion, the remaining residues accounted for 11.39, 9.49, and 11.9 % for heating rates of 5, 10, and 20 °C/min, respectively, for the T_5 pellet (Table 5). These results are consistent with those of other studies [93,94], although they employed different biomass sources. In summary, increasing the heating rate had a proportional effect on the combustion profile, suggesting that escalating the conversion's heating rate did not yield significantly advantageous results.

3.4. Temperature effect on thermal degradation in the combustion process

The thermal gravimetric (TG) analysis depicted in Figs 6 and 7 underscores the temperature-dependent nature of WSP's mass loss, with the extent of this loss intimately tied to temperature variations. Specifically, under the T_5 treatment and a heating rate of 20 °C/min, the mass loss registered at 6.1 % and 60.11 % within the temperature intervals of 25 to 297 °C, 397 to 527 °C, respectively. Beyond 527 °C, the TG curve exhibits a plateau-like profile, retaining 11.9 % of the initial mass under the same heating conditions. The T_5 pellet shows a parallel trend in mass loss, regardless of whether the heating rates are 10 or 5 °C/min (see Fig 6). In contrast, for T_1, weight loss was observed at 7 % and 86.29 % over the temperature ranges of 25 to 542 °C, respectively, using a 20 °C/min heating rate in an air environment. Nevertheless, weight loss becomes practically negligible after surpassing 542 °C, signifying a dearth of volatile constituents, while a residual mass of 6.71 % remains (Fig 7). These empirical findings align seamlessly with the scholarly work of Singh, Pandey [93].

The DTG profile fluctuation represents variation in the sample components [95]. Notably, the DTG profiles show identical peaks and several smaller side peaks across all types of pellets, irrespective of the applied heating rate. These observed distinctions could likely be attributed to elemental variations [96]. The highest peak signifies the point of most rapid reaction, occurring approximately within the temperature range of 200~325 °C. These findings align with prior research on using agricultural residues such as castor residue, maize cob, linseed stalks, and rice straw [97]. In the initial combustion stage, the decomposition rate is gradual, but as the temperature rises, the conversion rate accelerates. Beyond 542 °C, the reaction rate experiences a gradual decline (Figs. 6 and 7). In summary, it is evident that temperature

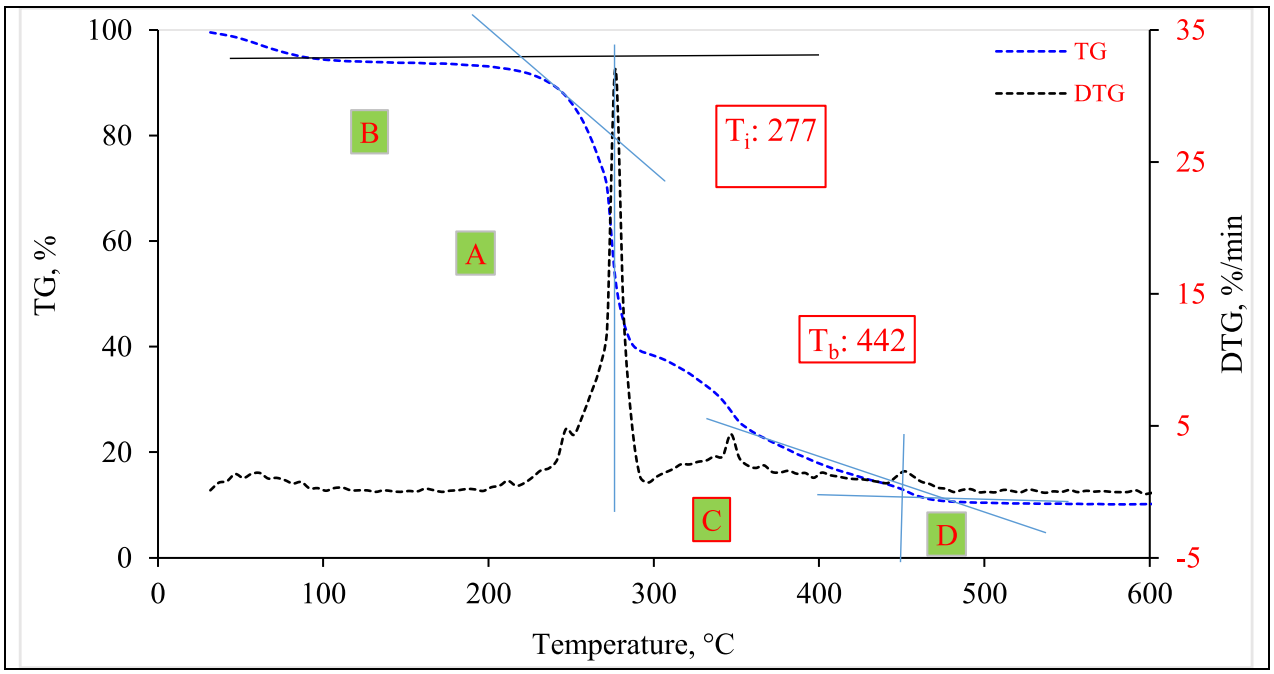

Fig. 10. TG and DTG curves for T_5 pellets at a constant heating rate of 10 °C/min.

Table 3
Combustion profile regions/phases/stages of wheat straw pellets [81].

Region/phase	I	II	III	IV
Name	Dehydration and desorption stage	Oxidation stage	Combustion stage	Burnout stage/Char combustion
Activities	Removal of moisture from below 110 °C	Removal of volatiles and adsorption/ absorption of oxygen, resulting in a mass loss in temperature zone 110~350 °C	Combustion of volatiles & and carbon content in temperature zone 350~550 °C	Combustion of lignin matter or gangues in temperature zone > 550 °C
Degradation component	Hemicellulose	Hemicellulose and cellulose		Lignin and charring

Table 4
Combustion characteristics of T_1 pellet at different heating rates.

Heating rate, °C/min	Item Trance,°C	Stage I 25–172	Stage II 172–332	Stage III 332–409	Stage IV 409–1200	Residue,%
20	T_{peak},°C	72	297	357	442	6.71
	M_{loss},%	7	54.15	22.72	9.42	
	DTG_{max},%/min	2.66	49.45	6.33	11.37	
10	T_{peak},°C	62	292	347	447	7.86
	M_{loss},%	6.66	56.64	15.74	13.1	
	DTG_{max},%/min	1.22	22.99	8.58	3.4	
5	T_{peak},°C	62	282	367	442	7.6
	M_{loss},%	6.96	60.13	17.08	8.23	
	DTG_{max},%.min^{-1}	0.86	9.02	1.51	1.38	

Note: T_{range}= Temperature range; T_{peak} = Peak/highest temperature; M_{loss} = Mass loss.
DTG_{max} = Maximum Differential Thermogravimetric/ maximum reaction rate.
Stage I= Mass losses occurred due to the moisture.
Stage II= Mass losses due to oxidative degradation (i.e., volatile released and then burned).
Stage III= Mass losses oxidative degradation (decompose of cellulose).
Stage IV= Mass losses combustion of the remaining char.

consistently influences specific decomposition reaction rates across all heating rates.

3.5. *Effect of additive addition in thermal combustion of wheat straw pellets*

Fig. 8 provides an illustrative representation of the TG profiles during the combustion of T_1 and T_5 pellets. Remarkably, both pellets follow a consistent behavior regardless of the applied heating rates. Initially, from the ambient temperature to approximately 207 °C, the TG curves for T_1 and T_5 almost coincide, regardless of heating rates (Fig. 8). Between 207 to 455 °C, it becomes evident that the T_5 pellet undergoes a relatively higher mass loss, approximately 8 %. Still, this disparity does not show significant variation across the range of heating rates. Alternatively, post 455 °C, the T_5 pellet experiences a higher mass loss, approximately 5 %. Interestingly, all three heating rates followed a

Table 5
Combustion characteristics of T_5 pellet at different heating rates.

Heating rate, °C/min	Item Trance,°C	Stage I 25~194	Stage II 194~297	Stage III 297~384	Stage IV 384~1200	Residue,%
20	T_{peak},°C	72	277	307	407	11.9
	M_{loss},%	6.1	60.11	11.72	10.17	
	DTG_{max},%/min	2.49	54.75	6.69	2.9	
10	T_{peak},°C	57	277	347	457	9.49
	M_{loss},%	6.7	56.59	15.53	11.69	
	DTG_{max},%/min	1.37	32.05	4.38	1.2	
5	T_{peak},°C	62	277	362	442	11.39
	M_{loss},%	6.64	55.08	17.02	9.87	
	DTG_{max},%/min	0.96	38.63	1.82	0.29	

parallel trend, and adding additives to expert no discernible impact on the thermal characteristics. Overall, the mass loss for both pellets remains remarkably consistent, indicating that the additive blending does not sustainably influence the combustion performance. This aligns with the findings in the study conducted by Ríos-Badrán [98], which focused on pellets made from rice husk, wheat straw and their blend.

The influence of additive blending on thermal combustion is elucidated through the DTG curve, as depicted in Fig. 9. Notably, the DTG profiles exhibit a striking similarity regardless of the applied heating rates, suggesting a uniform ash content. Research by Link, Yrjas [99] The influence of additive blending on thermal combustion is elucidated through the DTG curve, as depicted in Fig. 9. Notably, the DTG profiles exhibit a striking similarity regardless of the applied heating rates, suggesting a uniform ash content.

Conversely, the DTG_{max} temperature was comparatively lower for additive blended pellets (T_5) than those without additives (T_1) at heating rates ranging from 5 to 20 °C/min. For instance, at a heating rate of 10 °C/min, the T_5 pellet attains a maximum reaction rate of 32.05 %/min at 277 °C. In contrast, the T_1 pellet achieves a DTGmax of 22.99 %/min at 292 °C (refer to Fig. 9b). Interestingly, the DTGmax temperature for T_5 pellets remains constant at 277 °C, regardless of the heating rates, whereas peak temperatures vary for T_1 pellets. Moreover, the DTG profiles of T_1 and T_5 pellets exhibit distinctive peaks, further attesting to the impact of additives on enhancing conversion rates and suggesting a synergistic effect. Dhyani, Kumar [58] propose that including blending materials (such as coal, biomass and others) enhances fuel composition and boosts thermal properties. The present study findings concur with the research by Dhyani, Kumar [58] underscoring the positive impact of additives on wheat straw pellets' physical and compositional characteristics.

3.6. The ignition and burnout temperatures

The ignition temperature of biomass is critical in ensuring its safe handling during transportation and storage within various industries [100]. Conversely, a fuel's burnout temperature is a crucial indicator of its reaction extent and clean fuel [101]. According to [102], fuel components with lower volatility (hence less flammability) tend to exhibit higher burnout temperatures.

The intersection method was employed to ascertain wheat straw pellets' ignition and burnout temperatures (Figs. 10 and 11). For the T_5 wheat straw pellets, ignition occurred at 277 °C, followed by burnout at 442 °C, at a heating rate of 10 °C/min (Fig. 10). For the T_5 wheat straw pellets, ignition occurred at 277 °C, followed by burnout at 442 °C, at a heating rate of 10 °C/min.

Fig. 11 displays a visual representation of the thermal degradation progress of wheat straw pellets incorporating an additive blend (T_1), along with its corresponding derivative curve. The recorded ignition and burnout temperatures for T_1 pellets were 292 and 442 °C respectively, with a heating rate of 10 °C/min (Fig. 11). A recent study by Lu and

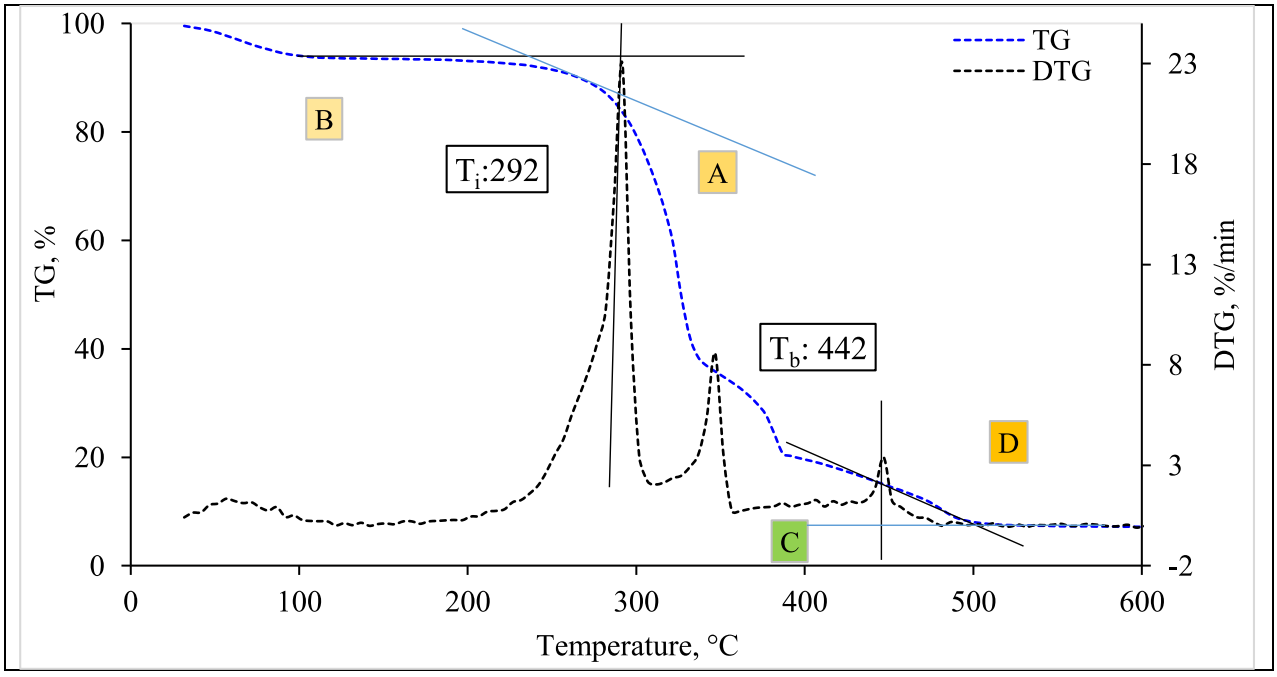

Fig. 11. TG and DTG curves for T_1 pellets at a constant heating rate of 10 °C/min.

Chen [55] delved into ignition and burnout temperatures for bamboo and sugarcanes using TGA, yielding burnout temperatures of 492 and 494 °C for bamboo and bagasse, respectively. The current investigation aligns with the outcomes of Lu and Chen [55]. Notably, the ignition point for T_1 pellets was consistently higher across all heating rates than T_5 pellets, while burnout temperatures were generally higher for T_5, except at 10 °C/min.

Table 6 provides a clear overview of the ignition and burnout temperatures across all pellet types, considering the three distinct heating rates. Notably, at a heating rate of 10 °C/min, two pellets show the highest ignition temperatures. Conversely, the T_1 pellet demonstrated a higher ignition temperature than T_5, indicating a notable difference. In the context of ignition temperatures, higher heating rates imply a more significant threshold for the ignition of the reaction [103]. In this study, incorporating additives into the wheat straw matrix may have contributed to an elevated ignition barrier, resulting in higher ignition temperatures. Alternatively, the burnout temperature was lowest at 10 °C/min among the various heating speeds. It is worth noting that a clear inverse relationship exists between ignition and burnout temperatures (Table 6).

3.7. Combustion characteristics indices

The combustion performance was comprehensively assessed through indices, including the Comprehensive Combustion Index (S), Flammability Index (C), Burnout Index (Db), and Ignition Point Index (Di), as outlined in Table 6. The combustion was more intense and burned faster when the S value was higher [104]. The combustion was more intense and burned faster when the S value was higher (Table 6). With the higher heating rate, both the flammability (C), ignition point (D_i) indices, and burnout point (D_b) indices sharply increased, but the ignition time (t_i) and burnout time (t_b) decreased. The greater Di value showed better ignition performance, and better combustion stability was established by the higher C value [10]. These results demonstrated that the increased heating rate greatly aided the WSP combustion's ignition and burnout performances. The findings were consistent with the research results of Zhang, Liu [12], even though they used cattle manure. For heating rates 5 and 10 °C/min, the S, D_i, and C were higher for the T_1 pellet than the T_5 pellets. Hence, higher heating rates enhanced the significant increases in S, Di, and C, indicating the energy potentiality of wheat straw pellets. However, for 20 °C/min heating rated, the D_i and C were higher for the T_5 pellets than the T_1 pellets. Galina, Luna [105] investigated the combustion characteristics of Pinus rice husk, sugarcane bagasse, and sorghum bagasse at oxy-fuel than air atmosphere. They found the same results as the present study.

3.8. Combustion efficiency of pellets

In this study, the combustion efficiency of pellets (T_1 and T_5) was assessed across a range of temperature variations from 300 to 700 °C, utilizing Eq. (5). It is observed from Fig. 12 it is evident that the efficiency (η) shows a notable upswing with an increase in temperature. Especially for T_1, the efficiency surged from 61.23 % to 98.52%, while for T_5 increased from 69.37 % to 99.14 % as the temperature increased from 300 to 700 °C. Notably, the combustion efficiency of WSP reached an impressive 99 %, similar to coal combustion efficiency (varied from 98.5 to 99.5 %) [106]. This similarity underscores the potential of wheat straw pellets as a viable bioenergy source. This increased efficiency with rising temperature can be attributed to higher volatilization of combustible material and concurrent combustion of VM and FC. The additive blend pellets (T_5) showed superior combustibility due to the lower moisture content, greater VM, oxygen, and higher levels of FC, hydrogen, and ash than T_1. Beyond 500 °C, both T_1 and T_5 showed comparable efficiency due to the near-complete combustion of (hemi) cellulose, as previously noted [12]. Overall, the experimental findings suggested that fuel should process higher hydrogen FC content for optimal combustion efficiency alongside lower moisture levels. On the other hand, higher ash reduces the combustion efficiency by reducing the available combustion material in the fuel.

4. Conclusion and outlook

This study aimed to identify the degradation stages and assess combustion indices for two variants of wheat straw pellets, denoted as T_1 and T_5, using Thermogravimetric Analysis (TGA). The findings can be summarised as follows:

- Wheat straw pellets exhibit higher volatile content and fuel ratio than coal. Their low nitrogen (N) and sulphur (S) levels suggest reduced NOx and SOx emissions. Their relatively high Higher Heating Value (HHV) and lower N/S content indicate their substantial potential as a clean and renewable energy source, albeit with distinctions from coal. When employing wheat straw as a biodiesel feedstock, attention should be given to slagging and ash deposition management.
- Physicochemical characterization reveals that pellets without additives (T_1) have lower heating values than those with additive blends

Table 6
Combustion characteristic parameters of wheat straw pellets.

Sample	β	T_i	T_p	T_b	- R_p	- R_v	t_i	t_p	t_b	S	D_i	D_b	C
T_1	5	251	442	462	60.13	1.25	50.2	88.4	92.4	19.94	1.35	1.47	9.54
	10	292	447	442	56.64	4.40	29.2	44.7	44.2	74.86	4.34	5.73	6.64
	20	267	442	467	54.15	6.78	13.35	22.1	23.35	148.30	18.35	20.99	7.60
T_5	5	233	442	456	38.63	1.02	46.6	88.4	91.2	11.62	0.94	0.96	7.12
	10	277	457	442	33.05	2.32	27.7	45.7	44.2	36.37	2.61	3.27	4.31
	20	207	407	492	54.75	4.03	10.35	20.35	24.6	104.66	25.99	21.87	12.78

Note:.
β = heating rate in °C/min.
R_p= maximum mass loss rate,%/min.
R_v= average mass loss rate,%/min.
S= comprehensive combustion index, 10^{-7} $\%^2/(min^2.\ °C^3)$.
D_i= ignition index, 10^{-2} $\%/min^3$.
C= flammability index, 10^{-4} $\%/(min.\ °C^2)$.
T_i= ignition temperature, **°C**.
T_p= peak temperature, **°C**.
T_b= burned-out temperature, **°C**.
t_i = ignition time, min.
t_p = peak reaction time, min.
t_b = burnout time, min.

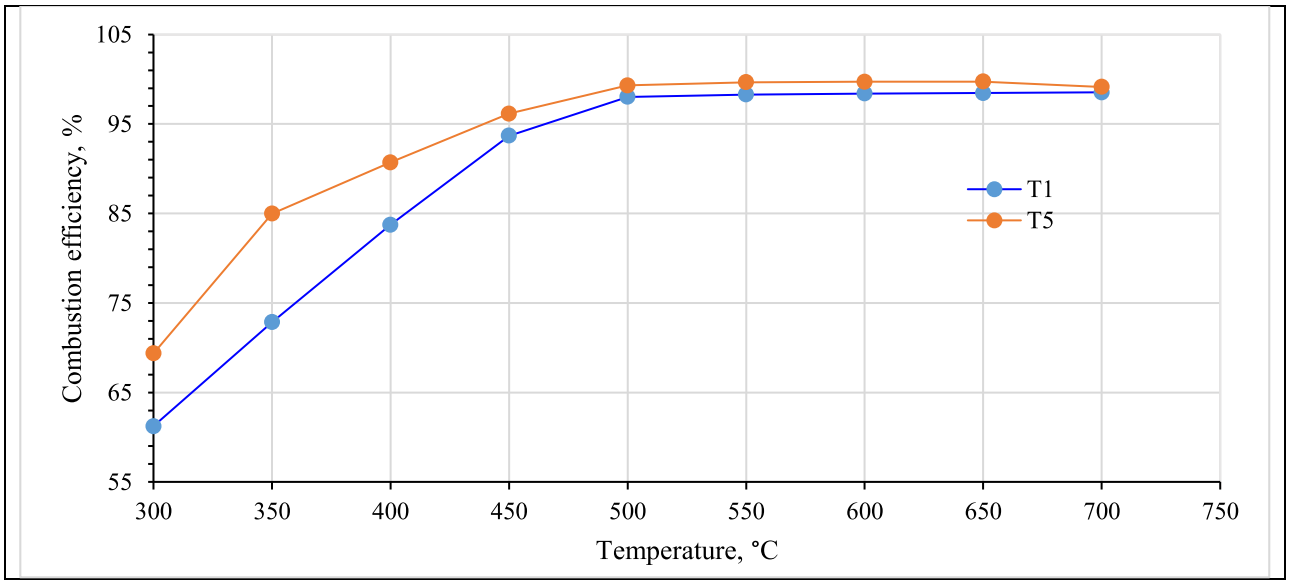

Fig. 12. Variation in combustion efficiency for wheat straw pellets.

(T_5), signifying significant enhancements in combustion properties through additive blending.

- The examination of TG/DTG profiles establishes that a heating rate of 20 °C/min is optimal, as it leads to higher mass loss and reaction rates for both pellet types.
- TG/DTG curves unveil four distinct stages in the degradation of Wheat Straw Pellets (WSP): devolatilization, oxidation, combustion, and subsequent burnout, leaving behind charred residual lignin.
- The results from TG analysis indicate that the thermal behaviour of WSP remains relatively consistent across different heating rates, differing notably from their mixture. The peak mass loss rate (reaction rate) shifts to a higher temperature in the DTG curve with increasing heating rates without altering the overall curve shape.
- Combustion parameter analysis reveals that the combustion of T_1 pellets presents more significant challenges than T_5. This underscores the effectiveness of additive blending in enhancing HHV, ignition, and combustion behaviour.
- Higher heating rates, particularly at 20 °C/min, significantly increase combustion indices and flammability, underscoring the considerable energy potential of wheat straw pellets.
- WSP's combustion efficiency reaches an impressive 99 % at 700 °C, comparable to coal's (which typically ranges from 98.5 to 99.5 %), affirming its status as a promising energy source.
- The experimental results obtained from this study will be valuable for TGA analysis of wheat straw pellets and other types of straw biomass, such as rice straw and barley straw.
- TGA has limitations in characterizing ash. In recognition of this constraint, our further investigation incorporates XRF and SEM analysis to provide a more comprehensive understanding of ash properties. For the identification of gas particles, experimentation based on TG-FTIR.

CRediT authorship contribution statement

Bidhan Nath: Writing – original draft, Visualization, Formal analysis, Data curation, Conceptualization. **Guangnan Chen:** Writing – review & editing, Supervision, Funding acquisition. **Les Bowtell:** Writing – review & editing, Supervision, Resources, Funding acquisition. **Elizabeth Graham:** Visualization, Validation, Data curation.

Declaration of competing interest

The authors declare that they have no known competing financial interests or personal relationships that could have appeared to influence the work reported in this paper.

Data availability

Data will be made available on request.

Acknowledgments

The authors thank the University of Southern Queensland (UniSQ), Australia, for its research facility. The National Agricultural Technology Program Phase-II, Bangladesh Agricultural Research Council (BARC), Farmgate, Dhaka 1215, Bangladesh, financially supported this work.

References

[1] S.A. Bandh, et al., Multidimensional analysis of global climate change: a review, Environ. Sci. Pollut. Res. 28 (20) (2021) 24872–24888.
[2] L.S. Budovich, Energy, exergy analysis in a hybrid power and hydrogen production system using biomass and organic Rankine cycle, Int. J. Thermofluids 21 (2024) 100584.
[3] X. Chen, Y. Liu, J. Wu, Sustainable production of formic acid from biomass and carbon dioxide, Mol. Catal. 483 (2020) 110716.
[4] B.I. Ali, D.G. Gunjo, Experimental and Numerical Investigation of throated downdraft gasifier using mango seed hull as a biomass, Int. J. Thermofluids (2024) 100608.
[5] P. Kumar, B.K. Nandi, Combustion characteristics of high ash Indian coal, wheat straw, wheat husk and their blends, Mater. Sci. Energy Technol. 4 (2021) 274–281.
[6] O. Erenstein, et al., *Global Trends in Wheat production, Consumption and trade*, in *Wheat improvement: Food Security in a Changing Climate*, Springer International Publishing Cham, 2022, pp. 47–66.
[7] S.H. Farjana, O. Tokede, M. Ashraf, Environmental impact assessment of waste wood-to-energy recovery in Australia, Energies (Basel) 16 (10) (2023) 4182.
[8] F. Hussin, et al., Environmental life cycle assessment of biomass conversion using hydrothermal technology: a review, Fuel Process. Technol. 246 (2023) 107747.
[9] J. Rivera, et al., Ignition of wildland fuels by idealized firebrands, Fire Saf. J. 120 (2021) 103036.
[10] R.K. Mishra, K. Mohanty, Kinetic analysis and pyrolysis behavior of low-value waste lignocellulosic biomass for its bioenergy potential using thermogravimetric analyzer, Mater. Sci. Energy Technol. 4 (2021) 136–147.
[11] J. Chen, et al., Investigation of co-combustion characteristics of sewage sludge and coffee grounds mixtures using thermogravimetric analysis coupled to artificial neural networks modeling, Bioresour. Technol. 225 (2017) 234–245.

[12] J. Zhang, et al., Kinetics, thermodynamics, gas evolution and empirical optimization of cattle manure combustion in air and oxy-fuel atmospheres, Appl. Therm. Eng. 149 (2019) 119–131.
[13] M.V. Kok, E. Özgür, Thermal analysis and kinetics of biomass samples, Fuel Process. Technol. 106 (2013) 739–743.
[14] H. Bi, et al., An experimental study of single unconventional biomass pellets: ignition characteristics, combustion processes, and artificial neural network modeling, Int. J. Energy Res. 44 (4) (2020) 2952–2965.
[15] F. Pan, et al., Analyzing temperature distribution patterns on the facing and backside surface: investigating combustion performance of flame-retardant particle boards using aluminum hypophosphite, intumescent, and magnesium hydroxide flame retardants, Polymers (Basel) 15 (23) (2023) 4479.
[16] Y. Ma, et al., Effects of solid acid and base catalysts on pyrolysis of rice straw and wheat straw biomass for hydrocarbon production, J. Energy Instit. 101 (2022) 140–148.
[17] H. Di, et al., Reactivity and catalytic effect of coals during combustion: thermogravimetric analysis, Energy 291 (2024) 130353.
[18] A. Petrovič, et al., Thermo-kinetic analysis of pyrolysis of thermally pre-treated sewage sludge from the food industry, Therm. Sci. Eng. Progr. 42 (2023) 101863.
[19] D. Kardaś, J. Kluska, P. Kazimierski, The course and effects of syngas production from beechwood and RDF in updraft reactor in the light of experimental tests and numerical calculations, Therm. Sci. Eng. Progr. 8 (2018) 136–144.
[20] C. Wang, et al., The thermal behavior and kinetics of co-combustion between sewage sludge and wheat straw, Fuel Process. Technol. 189 (2019) 1–14.
[21] M. Raza, et al., Isolation and characterization of cellulose from date palm waste using rejected brine solution, Int. J. Thermofluids 21 (2024) 100548.
[22] S. Szufa, et al., Torrefaction of oat straw to use as solid biofuel, an additive to organic fertilizers for agriculture purposes and activated carbon–TGA analysis, kinetics, in: E3S web of conferences, 2020.
[23] F. Sher, et al., Thermal and kinetic analysis of diverse biomass fuels under different reaction environment: a way forward to renewable energy sources, Energy Convers. Manage. 203 (2020).
[24] L. Xinjie, et al., Co-combustion of wheat straw and camphor wood with coal slime: thermal behaviour, kinetics, and gaseous pollutant emission characteristics, Energy 234 (2021) 121292.
[25] K.K. Dwivedi, M. Karmakar, P. Chatterjee, Thermal degradation, characterization and kinetic modeling of different particle size coal through TGA, Therm. Sci. Eng. Progr. 18 (2020) 100523.
[26] G. Cheng, et al., A comparative life cycle analysis of wheat straw utilization modes in China, Energy 194 (2020) 116914.
[27] A.U. Khan, et al., Characterization of fuel composite obtained by the mixing of biomass and coal, Energy Sources Part A Recov. Utiliz. Environ. Effects 46 (1) (2024) 2461–2473.
[28] L.V. Martínez, et al., Experimental study on the performance of gasification of corncobs in a downdraft fixed bed gasifier at various conditions, Renew. Energy 148 (2020) 1216–1226.
[29] S. Paniagua, A.I. García-Pérez, L.F. Calvo, Biofuel consisting of wheat straw–poplar wood blends: thermogravimetric studies and combustion characteristic indexes estimation, BioMass Convers. Biorefin. 9 (2) (2019) 433–443.
[30] P. Kumar, et al., Thermogravimetry and associated characteristics of pearl millet cob and eucalyptus biomass using differential thermal gravimetric analysis for thermochemical gasification, Therm. Sci. Eng. Progr. 26 (2021) 101104.
[31] S.A. El-Sayed, M. Khairy, An experimental study of combustion and emissions of wheat straw pellets in high-temperature air flows, Combust. Sci. Technol. (2017) 1–30.
[32] M. Lubwama, V.A. Yiga, Development of groundnut shells and bagasse briquettes as sustainable fuel sources for domestic cooking applications in Uganda, Renew. Energy 111 (2017) 532–542.
[33] I. Gageanu, et al., Impact of using additives on quality of agricultural biomass pellets, Eng. Rural Dev 17 (2018) 1632–1638.
[34] S. Emami, et al., Effect of fuel additives on agricultural straw pellet quality, Int. J. Agric. Biol. Eng. 7 (2) (2014) 92–100.
[35] J. Makwana, et al., An analysis of waste/biomass gasification producing hydrogen-rich syngas: a review, Int. J. Thermofluids (2023) 100492.
[36] T. Emiola-Sadiq, L. Zhang, A.K. Dalai, Thermal and kinetic studies on biomass degradation via thermogravimetric analysis: a combination of model-fitting and model-free approach, ACS. Omega 6 (34) (2021) 22233–22247.
[37] H. Khan, S. Savvopoulos, I. Janajreh, Artificial neural network-assisted thermogravimetric analysis of thermal degradation in combustion reactions: a study across diverse organic samples, Environ. Res. (2024) 118463.
[38] O. Al-Ayed, W. Saadeh, Approaches to biomass kinetic modelling: thermochemical biomass conversion processes, Jordan. J. Eng. Chem. Ind. 4 (1) (2021).
[39] B. Nath, et al., Kinetic mechanism of wheat straw pellets combustion process with a thermogravimetric analyser, Heliyon 9 (10) (2023).
[40] P. Pradhan, S.M. Mahajani, A. Arora, Production and utilization of fuel pellets from biomass: a review, Fuel Process. Technol. 181 (2018) 215–232.
[41] M. Nazemi, et al., Producing high-strength pellets from seaweed, sawdust, and hay for gasification, in: ASME International Mechanical Engineering Congress and Exposition, American Society of Mechanical Engineers, 2022.
[42] L.G. Tabil, Binding and pelleting characteristics of alfalfa. Department of Agricultural and Bioresource Engineering, University of Saskatchewan, Saskatoon, Saskatchewan, CA, 1996.
[43] B. Nath, et al., Assessment of densified fuel quality parameters: a case study for wheat straw pellet, J. Bioresour. Bioprod. 8 (1) (2023) 45–58.
[44] ISO/TS. *17225-8: solid biofuels - Fuel specifications and classes - Part 8: graded thermally treated and densified biomass fuels*. 2016; Available from: https://www.iso.org/standard/71915.html.
[45] R. Rioux, et al., High-surface-area catalyst design: synthesis, characterization, and reaction studies of platinum nanoparticles in mesoporous SBA-15 silica, J. Phys. Chem. B 109 (6) (2005) 2192–2202.
[46] S. Barbhuiya, B.B. Das, F. Kanavaris, Biochar-concrete: a comprehensive review of properties, production and sustainability, Case Stud. Constr. Mater. (2024) e02859.
[47] M. Jeguirim, G. Trouvé, Pyrolysis characteristics and kinetics of Arundo donax using thermogravimetric analysis, Bioresour. Technol. 100 (17) (2009) 4026–4031.
[48] M. Carrier, et al., Thermogravimetric analysis as a new method to determine the lignocellulosic composition of biomass, Biomass Bioenergy 35 (1) (2011) 298–307.
[49] I. Ali, H. Bahaitham, R. Naebulharam, A comprehensive kinetics study of coconut shell waste pyrolysis, Bioresour. Technol. 235 (2017) 1–11.
[50] N. Vhathvarothai, J. Ness, Q.J. Yu, An investigation of thermal behaviour of biomass and coal during copyrolysis using thermogravimetric analysis, Int. J. Energy Res. 38 (9) (2014) 1145–1154.
[51] P. Rex, L.R. Miranda, Catalytic activity of acid-treated biomass for the degradation of expanded polystyrene waste, Environ. Sci. Pollut. Res. 27 (1) (2020) 438–455.
[52] N. Manić, B. Janković, V. Dodevski, Model-free and model-based kinetic analysis of Poplar fluff (Populus alba) pyrolysis process under dynamic conditions, J. Therm. Anal. Calorim. 143 (5) (2021) 3419–3438.
[53] J.Y. Yeo, et al., Comparative studies on the pyrolysis of cellulose, hemicellulose, and lignin based on combined kinetics, J. Energy Instit. 92 (1) (2019) 27–37.
[54] F.G. Fonseca, et al., Challenges in kinetic parameter determination for wheat straw pyrolysis, Energies (Basel) 15 (19) (2022) 7240.
[55] J.-J. Lu, W.-H. Chen, Investigation on the ignition and burnout temperatures of bamboo and sugarcane bagasse by thermogravimetric analysis, Appl. Energy 160 (2015) 49–57.
[56] Q. Yi, et al., Thermogravimetric analysis of co-combustion of biomass and biochar, J. Therm. Anal. Calorim. 112 (3) (2013) 1475–1479.
[57] R. Kaur, et al., Pyrolysis kinetics and thermodynamic parameters of castor (Ricinus communis) residue using thermogravimetric analysis, Bioresour. Technol. 250 (2018) 422–428.
[58] V. Dhyani, J. Kumar, T. Bhaskar, Thermal decomposition kinetics of sorghum straw via thermogravimetric analysis, Bioresour. Technol. 245 (2017) 1122–1129.
[59] F. Shan, et al., An experimental study of ignition and combustion of single biomass pellets in air and oxy-fuel, Fuel 188 (2017) 277–284.
[60] S.-W. Du, W.-H. Chen, J. Lucas, Performances of pulverized coal injection in blowpipe and tuyere at various operational conditions, Energy Convers. Manage 48 (7) (2007) 2069–2076.
[61] B. Arias, et al., Effect of biomass blending on coal ignition and burnout during oxy-fuel combustion, Fuel 87 (12) (2008) 2753–2759.
[62] L. Tognotti, et al., Measurement of ignition temperature of coal particles using a thermogravimetric technique, Combust. Sci. Technol. 44 (1–2) (1985) 15–28.
[63] L.C.d. Morais, et al., Thermochemical conversion of sugarcane bagasse: a comprehensive analysis of ignition and burnout temperatures, Clean Technol. 4 (4) (2022) 1127–1137.
[64] Z. Liu, et al., Thermogravimetric investigation of hydrochar-lignite co-combustion, Bioresour. Technol. 123 (2012) 646–652.
[65] M. Soh, et al., Comprehensive kinetic study on the pyrolysis and combustion behaviours of five oil palm biomass by thermogravimetric-mass spectrometry (TG-MS) analyses, Bioenergy Res. 12 (2) (2019) 370–387.
[66] J. Hu, et al., Combustion behaviors of three bamboo residues: gas emission, kinetic, reaction mechanism and optimization patterns, J. Clean. Prod. 235 (2019) 549–561.
[67] G. Sun, et al., (Co-) combustion behaviors and products of spent potlining and textile dyeing sludge, J. Clean. Prod. 224 (2019) 384–395.
[68] C. Xie, et al., Quantifying thermal decomposition regimes of textile dyeing sludge, pomelo peel, and their blends, Renew. Energy 122 (2018) 55–64.
[69] B. Nath, et al., Assessment of densified fuel quality parameters: a case study for wheat straw pellet, J. Bioresour. Bioprod. (2022).
[70] T. Wang, et al., Combustion behavior of refuse-derived fuel produced from sewage sludge and rice husk/wood sawdust using thermogravimetric and mass spectrometric analyses, J. Clean. Prod. 222 (2019) 1–11.
[71] J. Huang, et al., Combustion behaviors of spent mushroom substrate using TG-MS and TG-FTIR: thermal conversion, kinetic, thermodynamic and emission analyses, Bioresour. Technol. 266 (2018) 389–397.
[72] V. Dhyani, T. Bhaskar, A comprehensive review on the pyrolysis of lignocellulosic biomass, Renew. Energy 129 (2018) 695–716.
[73] M. Hu, et al., Kinetic study and syngas production from pyrolysis of forestry waste, Energy Convers. Manage. 135 (2017) 453–462.
[74] G. Ye, et al., Evaluating the bioenergy potential of Chinese Liquor-industry waste through pyrolysis, thermogravimetric, kinetics and evolved gas analyses, Energy Convers. Manage. 163 (2018) 13–21.
[75] M. Mureddu, et al., Air-and oxygen-blown characterization of coal and biomass by thermogravimetric analysis, Fuel 212 (2018) 626–637.
[76] H. Song, G. Liu, J. Wu, Pyrolysis characteristics and kinetics of low rank coals by distributed activation energy model, Energy Convers. Manage 126 (2016) 1037–1046.

[77] F. Guo, Z. Zhong, Optimization of the co-combustion of coal and composite biomass pellets, J. Clean. Prod. 185 (2018) 399–407.
[78] Y. Rahib, et al., Experimental analysis on thermal characteristics of argan nut shell (ANS) biomass as a green energy resource, Int. J. Renew. Energy Res. 9 (4) (2019) 1606–1615.
[79] Z. Yao, X. Ma, Characteristics of co-hydrothermal carbonization on polyvinyl chloride wastes with bamboo, Bioresour. Technol. 247 (2018) 302–309.
[80] R.K. Mishra, K. Mohanty, Kinetic analysis and pyrolysis behaviour of waste biomass towards its bioenergy potential, Bioresour. Technol. 311 (2020) 123480.
[81] J. Zhao, et al., Assessing the effectiveness of a high-temperature-programmed experimental system for simulating the spontaneous combustion properties of bituminous coal through thermokinetic analysis of four oxidation stages, Energy 169 (2019) 587–596.
[82] M.S. Ahmad, et al., Bioenergy potential of Wolffia arrhiza appraised through pyrolysis, kinetics, thermodynamics parameters and TG-FTIR-MS study of the evolved gases, Bioresour. Technol. 253 (2018) 297–303.
[83] Xu, Q., *Investigation of co-gasification characteristics of biomass and coal in fluidized bed gasifiers.* 2013.
[84] A. Alvarez, et al., Determination of kinetic parameters for biomass combustion, Bioresour. Technol. 216 (2016) 36–43.
[85] L. Liu, et al., Thermal and kinetic analyzing of pyrolysis and combustion of self-heating biomass particles, Process Saf. Environ. Prot. 151 (2021) 39–50.
[86] T. Xie, et al., Comparative analysis of thermal oxidative decomposition and fire characteristics for different straw powders via thermogravimetry and cone calorimetry, Process Saf. Environ. Prot. 134 (2020) 121–130.
[87] Y. Gao, et al., Factors affecting the yield of bio-oil from the pyrolysis of coconut shell, Springerplus 5 (1) (2016) 1–8.
[88] Z. Hameed, et al., A comprehensive review on thermal coconversion of biomass, sludge, coal, and their blends using thermogravimetric analysis, J. Chem. 2020 (2020) 1–23.
[89] A.S. Qureshi, et al., Fruit waste to energy through open fermentation, Energy Procedia 142 (2017) 904–909.
[90] H.H. Sait, et al., Pyrolysis and combustion kinetics of date palm biomass using thermogravimetric analysis, Bioresour. Technol. 118 (2012) 382–389.
[91] B. Gajera, et al., Impact of torrefaction on thermal behavior of wheat straw and groundnut stalk biomass: kinetic and thermodynamic study, Fuel Commun. 12 (2022) 100073.
[92] M. Asadieraghi, W.M.A.W. Daud, Characterization of lignocellulosic biomass thermal degradation and physiochemical structure: effects of demineralization by diverse acid solutions, Energy Convers. Manage. 82 (2014) 71–82.
[93] R.K. Singh, et al., Pyrolysis of banana leaves biomass: physico-chemical characterization, thermal decomposition behavior, kinetic and thermodynamic analyses, Bioresour. Technol. 310 (2020) 123464.
[94] K. Açıkalın, Determination of kinetic triplet, thermal degradation behaviour and thermodynamic properties for pyrolysis of a lignocellulosic biomass, Bioresour. Technol. 337 (2021) 125438.
[95] T. Yan, et al., Investigation on the synergistic effect between different components in pyrolysis of paper-plastic composite material, J. Anal. Appl. Pyrolysis 177 (2024) 106337.
[96] G.K. Gupta, M.K. Mondal, Kinetics and thermodynamic analysis of maize cob pyrolysis for its bioenergy potential using thermogravimetric analyzer, J. Therm. Anal. Calorim. 137 (4) (2019) 1431–1441.
[97] W.-H. Chen, et al., Torrefaction, pyrolysis and two-stage thermodegradation of hemicellulose, cellulose and lignin, Fuel 258 (2019) 116168.
[98] I.M. Ríos-Badrán, et al., Production and characterization of fuel pellets from rice husk and wheat straw, Renew. Energy 145 (2020) 500–507.
[99] S. Link, P. Yrjas, L. Hupa, Ash melting behaviour of wheat straw blends with wood and reed, Renew. Energy 124 (2018) 11–20.
[100] M. Calabrese, et al., Hydrogen safety challenges: a comprehensive review on production, storage, transport, utilization, and CFD-based consequence and risk assessment, Energies (Basel) 17 (6) (2024) 1350.
[101] A.T. Kole, et al., Design, development, and performance evaluation of husk biomass cook stove at high altitude condition, Int. J. Thermofluids 16 (2022) 100242.
[102] C.-Y. Hsuan, S.-S. Hou, Co-combustion characteristics and kinetics of sludge/coal blends in 21%–50% oxygen-enriched O2/CO2 atmospheres, Fuel 362 (2024) 130821.
[103] W. Cao, et al., Experimental study on the ignition characteristics of cellulose, hemicellulose, lignin and their mixtures, J. Energy Instit. 92 (5) (2019) 1303–1312.
[104] X. Liu, et al., Hydrogen pre-chamber combustion at lean-burn conditions on a heavy-duty diesel engine: a computational study, Fuel 335 (2023) 127042.
[105] N.R. Galina, et al., Comparative study on combustion and oxy-fuel combustion environments using mixtures of coal with sugarcane bagasse and biomass sorghum bagasse by the thermogravimetric analysis, J. Energy Instit. 92 (3) (2019) 741–754.
[106] F. Guo, Z. Zhong, Co-combustion of anthracite coal and wood pellets: thermodynamic analysis, combustion efficiency, pollutant emissions and ash slagging, Environ. Pollut. 239 (2018) 21–29.